JOURNAL OF
NON-CRYSTALLINE SOLIDS

Journal of Non-Crystalline Solids 195 (1996) 148–157

Effect of Pt doping on nucleation and crystallization in $Li_2O \cdot 2SiO_2$ glass: experimental measurements and computer modeling

K. Lakshmi Narayan [a], K.F. Kelton [a,*], C.S. Ray [b]

[a] *Department of Physics, Washington University, Box 1105, 1 Brookings Drive, St. Louis MO 63130, USA*
[b] *Graduate Center for Materials Research, University of Missouri–Rolla, Rolla, MO 65401, USA*

Received 29 March 1995; revised 21 August 1995

ELSEVIER

JOURNAL OF NON-CRYSTALLINE SOLIDS

A journal on the chemical, electronic, optical, and mechanical properties of glasses, amorphous semiconductors and metals, sol–gel materials, the liquid state of these solids, and the processes by which they are formed.

(for complete addresses, see page 2 of the preliminary pages)

Aims and Scope
Review Articles, Research Papers, Comments and Letters on chemical, electronic, optical, mechanical, structural and fracture properties of non-crystalline materials including glasses, amorphous semiconductors, metals (alloys) and sol–gel materials which form glasses, the liquid state of all materials from which non-crystalline solids can be formed, and the processes for the formation of non-crystalline solids are accepted.

Abstracted/indexed in:
Biological Abstracts; Ceramic Abstracts; Current Contents: Engineering, Technology and Applied Sciences; EI Compendex Plus; Engineered Materials Abstracts; Engineering Index; INSPEC; Metals Abstracts; Physics Briefs.

Subscription Information 1996
Volumes 192–207 of Journal of Non-Crystalline Solids (ISSN 0022-3093) are scheduled for publication. (Frequency: monthly.) Prices are available from the publishers upon request. Subscriptions are accepted on a prepaid basis only and are entered on a calendar-year basis. Issues are sent by SAL (surface air lifted) mail wherever this service is available. Airmail rates are available upon request. Please address all enquiries regarding orders and subscriptions to:

Elsevier Science B.V.
Order Fulfilment Department
PO Box 211, 1000 AE Amsterdam
The Netherlands
Tel: +31-20 485 3642, Fax: +31-20 485 3598.

Claims for issues not received should be made within six months of our publication (mailing) date. If not, they cannot be honoured free of charge.

US Mailing notice – Journal of Non-Crystalline Solids (ISSN 0022-3093) is published monthly, except semimonthly in February, March, May, June, July and August, by Elsevier Science B.V., Molenwerf 1, P.O. Box 211, 1000 AE Amsterdam, The Netherlands. Annual subscription price in the USA is US$ 4654 (valid in North, Central and South America only), including air speed delivery. Second class postage paid at Jamaica, NY 11431.
USA Postmasters: Send changes to Journal of Non-Crystalline Solids, Publications Expediting, Inc., 200 Meacham Avenue, Elmont, NY 11003. Airfreight and mailing in the USA by Publications Expediting.

♾ The paper used in this publication meets the requirements of ANSI/NISO 239.48-1992 (Permanence of Paper).

North-Holland, an imprint of Elsevier Science

ELSEVIER

Journal of Non-Crystalline Solids 195 (1996) 148–157

JOURNAL OF NON-CRYSTALLINE SOLIDS

Effect of Pt doping on nucleation and crystallization in $Li_2O \cdot 2SiO_2$ glass: experimental measurements and computer modeling

K. Lakshmi Narayan [a], K.F. Kelton [a,*], C.S. Ray [b]

[a] *Department of Physics, Washington University, Box 1105, 1 Brookings Drive, St. Louis MO 63130, USA*
[b] *Graduate Center for Materials Research, University of Missouri–Rolla, Rolla, MO 65401, USA*

Received 29 March 1995; revised 21 August 1995

Abstract

Heterogeneous nucleation and its effects on the crystallization of lithium disilicate glass containing small amounts of Pt are investigated. Measurements of the nucleation frequencies and induction times with and without Pt are shown to be consistent with predictions based on the classical nucleation theory. A realistic computer model for the transformation is presented. Computed differential thermal analysis data (such as crystallization rates as a function of time and temperature) are shown to be in good agreement with experimental results. This modeling provides a new, more quantitative method for analyzing calorimetric data.

1. Introduction

For many reasons, lithium disilicate glass provides a model system for studying nucleation and crystallization in glasses. Good experimental data exist for steady-state and time-dependent nucleation rates and growth velocities [1–3]. Further, the free energy differences between the glass and the crystal are available as a function of temperature [4]. These data have been used extensively to test the classical theory for homogeneous nucleation [5,6] and its extensions to describe polymorphic growth [7]. Further, those kinetic models have been used to simulate crystallization in this glass under isothermal and non-isothermal conditions [8,9]. Possible extensions to treat crystallization that is nucleated heterogeneously on glass impurities have also been considered [10,11].

It is well known that the addition of noble metals in controlled quantities increases the tendency for glasses to nucleate. Rindone [12], for example, demonstrated the effectiveness of platinum particles in precipitating lithium disilicate crystals from lithium disilicate glass. Cronin and Pye [13] have investigated the effect of Pt particle size on the crystallization of lithium disilicate glass. Heterogeneous or catalyzed nucleation, however, has received less theoretical attention than has homogeneous nucleation. This is primarily due to insufficient information about the number, size and catalytic efficiency of the heterogeneous particles. By conducting quantitative investigations on metallic and silicate glasses, Kelton

* Corresponding author. Tel: +1-314 935 6228. Telefax: +1-314 935 6219. E-mail: kfk@wuphys.wustl.edu.

SSDI 0022-3093(95)00526-9

and Greer [6,14] demonstrated previously that detailed studies of the transient nucleation rates provide more information about the nucleation process than is available from the study of steady-state rates alone. Surprisingly, only a few measurements of the time-dependent heterogeneous nucleation rates in silicate glasses exist [15].

Here, we present measurements of heterogeneous nucleation rates in lithium disilicate glass as a function of Pt concentration. Both time-dependent and steady-state nucleation rates are measured at each Pt concentration, and the nucleation induction times are determined. Similar measurements were also conducted on an undoped glass to compare the quantitative effects of homogeneous and heterogeneous nucleation on the crystallization of the lithium disilicate glass. The computer model developed for homogeneous nucleation is extended to include the effect of heterogeneities [10] and is used to analyze the experimental data.

A numerical model previously developed to provide a description of polymorphic crystallization for glasses heated at a constant rate, such as is used in differential scanning calorimetry (DSC) or differential thermal analysis (DTA) experiments, is extended to include heterogeneous nucleation. Exothermic crystallization peaks were measured and were modeled as a function of dopant (Pt) concentration and the heating rate. The applicability of the Kissinger method [26] for extracting an overall activation energy for crystallization was also evaluated.

2. Theoretical background

Nucleation is normally modeled assuming the classic theory of nucleation, in which clusters of various sizes exist simultaneously, growing or shrinking as governed by a series of bimolecular rate equations, describing the addition and loss of a single manomer per step. Assuming a sharp interface, the reversible work of formation of a cluster of size n is the sum of a volume term (which is negative for the phase transformation to proceed) and a positive energetic penalty for the introduction of a surface:

$$W_n = n\,\Delta G + \alpha n^{2/3}\sigma. \tag{1}$$

Here ΔG is the free energy difference per molecule between the crystal and the glass, α is a geometrical factor and σ is the interfacial energy between the crystal and the glass. The barrier to nucleation is decreased if the nucleating cluster wets the catalyzing impurity. Within the spherical cap model for heterogeneous nucleation, the interfacial energy is decreased from its value for homogeneous nucleation, σ_0,

$$\sigma^3 = f(\phi)\,\sigma_0^3, \tag{2}$$

where

$$f(\phi) = \left[(2+\cos\phi)(1-\cos\phi)^2\right]/4. \tag{3}$$

Here ϕ is the contact angle between the growing crystal nucleus and the heterogeneous impurity. Following a sufficiently long time, the cluster distribution will approach the steady-state distribution, which is characterized by the temperature and the thermodynamic and kinetic constants but is independent of time and sample thermal history. Due to the quenching process, however, nucleation in most glasses is not initially at its steady-state value but approaches it with time as the cluster distribution approaches its constant value [8,9]. The rate of change in the cluster density is given by

$$\frac{\mathrm{d}N_{n,t}}{\mathrm{d}t} = k^+_{n-1}N_{n-1,t} - \left[k^+_n + k^-_n\right]N_{n,t} + k^-_{n+1}N_{n+1,t}, \tag{4}$$

where k^+_n and k^-_n are the rates at which molecules join or leave clusters of n molecules, giving a time- and cluster-size-dependent nucleation rate

$$I_{n,t} = N_{n,t}k^+_n - N_{n+1,t}k^-_{n+1}. \tag{5}$$

Following Turnbull and Fischer [16], the atomic attachment and detachment frequencies, respectively, are

$$k^+_n = O_n\gamma\exp\left(\frac{W_n - W_{n+1}}{2k_BT}\right), \tag{6}$$

$$k^-_{n+1} = O_{n+1}\gamma\exp\left(\frac{W_{n+1} - W_n}{2k_BT}\right),$$

where k_B is the Boltzmann's constant, O_n is the number of sites available for the attachment of a monomer and γ is an unbiased jump frequency that

can be expressed in terms of the diffusion coefficient, D, and the average jump distance, λ,

$$\gamma = 6D/\lambda^2. \tag{7}$$

In silicate glasses, the nucleation rate is determined by first annealing the sample at a temperature at which the nucleation rate is large and the growth velocity is small, followed by an anneal at a higher temperature at which the nucleation rate is negligible, but the growth velocity is substantial. During the growth treatment, all clusters larger than the critical size at that temperature, n_G^*, will grow [3,15]. To compare theory with experiment, the cluster size, n, in Eq. (5) is, therefore, typically chosen equal to n_G^*. The measured quantity is the number of nuclei, $N(T,t)$, produced as a function of time; its time derivative is the nucleation rate, $I(t,T)$. Under steady-state conditions, the slope of N vs. t is equal to the steady-state nucleation rate, I^s. Experiments on quenched glasses typically give a nucleation rate that is lower than I^s; that value is approached asymptotically with time. At long times,

$$N(T,t) = I^s(t-\theta), \tag{8}$$

where θ, the effective time-lag, depends upon the particular glass system and temperature, T, and I^s is the steady-state nucleation rate.

While often not discussed, heterogeneous nucleation can also display transient behavior. This can be easily seen with only minor modifications to the development for homogeneous nucleation. The work of cluster formation is changed, as already discussed. The number of surface attachment sites is decreased,

$$O_n \rightarrow O_n[f(\theta)]^{2/3} \tag{9}$$

which, according to Eq. (6), decreases the atomic attachment and detachment frequency, as well.

3. Computer simulation of crystallization

The details of the numerical model for crystallization under non-isothermal conditions have been discussed elsewhere [8,9]. With the changes mentioned in the previous section, the model can be directly applied to describe crystallization by heterogeneous nucleation. As before, the non-isothermal scan is divided into a series of isothermal anneals, the duration of which, Δt, is set by the coarseness of the temperature step, ΔT, and the scan rate, Q:

$$\Delta t = \Delta T/Q. \tag{10}$$

Within each isothermal interval, the clusters are allowed to evolve following the bimolecular rate kinetics of the classical theory of nucleation, using the kinetic and thermodynamic factors appropriate to the temperature of that interval. To include the effect of heterogeneous nucleation, the work of cluster formation and the rate constants are adjusted using Eqs. (2) and (9), respectively. This is accomplished by further dividing each isothermal interval into finer time steps, δt, and using a finite difference approach to solve the coupled kinetic equations of nucleation, i.e., Eqs. (4) and (5). The cluster density as a function of time is computed by

$$N_{n,t+\delta t} = N_{n,t} + \delta t(\mathrm{d}N_{n,t}/\mathrm{d}t), \tag{11}$$

where $\mathrm{d}N_{n,t}$ is determined from Eq. (4). The time-dependent nucleation rate is, therefore, calculated from Eq. (5), avoiding the introduction of ad hoc assumptions regarding its behavior. At the end of each isothermal interval, the clusters generated during that isothermal anneal and those generated during the previous isothermal intervals are grown using the appropriate cluster-size-dependent growth velocity [9,17]

$$g(r) = \frac{16CD}{\lambda^2}\left(\frac{3\bar{\nu}}{4\pi}\right)^{1/3} \sinh\left[\frac{\bar{\nu}}{2k_B T}\left(\Delta G_v - \frac{2\sigma}{r}\right)\right]. \tag{12}$$

As was demonstrated previously [7], the temperature dependence of the macroscopic growth rate calculated from Eq. (12) using thermodynamic and kinetic parameters derived from nucleation data (appropriate for the growth of small clusters) is in good agreement with experimental results. The magnitudes of the calculated values, however, are too low. This is likely due to a relatively temperature-independent anisotropic growth mechanism that causes an increase in the number of attachment sites on the larger clusters (see Ref. [7] for more detail). For the computer calculations presented here, C was set to 4.77 to give good agreement with the observed macroscopic crystal growth rates. Keeping track of the number of clusters of a given size, $r_{i,t}$, and

Table 1
Parameters for the simulation of crystallization of lithium disilicate

Melting temperature, T_m:	1300 K
Molecular volume, V_{mol}:	9.962×10^{-29} m^3
Entropy of fusion, ΔS_f:	39.08 kJ mol^{-1} K^{-1}
Interfacial energy for homogeneous nucleation, σ:	$(0.094+7\times10^{-5}\ T)$ J m^{-2}
Jump distance, λ:	4.6 Å
Diffusion coefficient:	$D = D_0 T \exp\left(\frac{b}{T_0 - T}\right)$
D_0:	3.63×10^{-14} m^2 K^{-1} s^{-1}
b:	7761 K
T_0:	460 K
Gibbs free energy (J mol^{-1}):	$\Delta G = a_0 + a_1 T + a_2 T^2 + a_3 T^3$
a_0:	48045 J mol$_{-1}$
a_1:	-36.81 J mol^{-1} K^{-1}
a_2:	5.607×10^{-3} J mol^{-1} K^{-2}
a_3:	-4.3179×10^{-6} J mol^{-1} K^{-3}

assuming no overlap between the clusters, the total extended volume transformed is calculated directly as

$$x_e = \frac{4\pi}{3V_0} \sum_i N_i r_{i,t}^3. \tag{13}$$

Cluster overlap is taken into account statistically using the Johnson–Mehl–Avrami equation [28] to relate the actual volume fraction transformed to the extended volume fraction transformed:

$$x = 1 - \exp(-x_e). \tag{14}$$

Assuming that the DSC signal scales with the rate of volume fraction transformed,

$$\text{DSC signal} \propto \left[x(T_i + \delta T) - x(T_i)\right]/\delta t. \tag{15}$$

The physical parameters used in the calculations of nucleation and growth in lithium disilicate glass are given in Table 1.

4. Experimental procedure

Samples of lithium disilicate glass were prepared with differing amounts of Pt to act as heterogeneous sites. These were annealed and the rate of nuclei production was measured to determine time-dependent nucleation rates. Experimental DSC scans were made to determine the effect of these heterogeneities on the overall transformation behavior. In this section, experimental procedures are discussed.

4.1. Glass preparation

A well mixed, 50 g batch of lithium disilicate composition was melted in a platinum crucible at 1450 C for 2 h, and the melt was cast between two steel plates. Chloroplatinic acid was used in the batch to prepare glasses containing platinum. Before casting, the melt was stirred periodically (25–30 min interval) with a silica rod to ensure homogeneity. X-ray diffraction and examination by scanning electron microscopy (SEM) showed no evidence of unmelted or crystalline particles in the as-quenched glass. Glasses containing 0 (undoped), 1, 5, 10 and 50 ppm nominal concentration of Pt by weight were prepared and used in the present investigation. To avoid moisture contamination, all glasses were stored in a vacuum desiccator until used for measurements.

4.2. Nucleation rate measurements

Glasses containing 0 (undoped), 1 and 5 ppm Pt of dimensions ≈ 1 cm $\times$ 1 cm $\times$ 4 mm were used for nucleation rate measurements. They were placed in a tube furnace capable of maintaining the temperature to ± 1 C. To determine the nucleation kinetics, the glasses were nucleated over a temperature range from 432 to 500°C, and then grown at 700°C for 3 min, following James [15].

The annealed samples were ground and polished to remove effects due to surface crystallization. They were lightly etched for 15 s in a 3% HF, 4% HNO_3 solution prepared in deionized water. The samples were then analyzed in an optical microscope (Leitz–Wetzlar, type Metallux-3) at magnifications up to 1000 times. Standard stereologic corrections were applied to determine the crystal density per unit volume [18]. Assuming that each crystal grows from a single nucleus and that no nuclei larger than the critical size at the growth temperature re-dissolve in the second stage anneal, the number of visible clusters present in a unit volume of the sample corresponds to the number of nuclei per unit volume, N_v.

By measuring the number of nuclei, N_v^0, present in a non-nucleated as-quenched glass, the number of nuclei generated per unit volume during an annealing period was determined as $N = N_v - N_v^0$.

Attempts to determine platinum concentration and cluster sizes were made using SEM (Hitachi 4000GL) and transmission electron microscopy (JEOL 2000FX).

4.3. DTA studies

All of the calorimetric data were obtained in a flowing argon atmosphere (40 cm^3/min) using a Perkin–Elmer DTA 1700 system. Samples weighing between 15 and 20 mg were ground and heated in a Pt crucible until crystallization was complete. To minimize surface crystallization effects, particles approximately 1 mm in diameter were used. Scans were made at 5, 10, 20, 40 and 80°C/min, respectively, on all samples. High purity Al_2O_3 was used as the reference material. Instrumental shifts in temperature were corrected by measuring the melting point of aluminum as a function of the scan rate. These experimental DTA exotherms were then compared with those simulated using identical sample characteristics and heating rates in the computer model.

5. Results and discussion

Direct measurements of the nucleation rates and induction times were made to obtain estimates of the contact angles and to check predictions of the theories. Data from these nucleation measurements were used to compute non-isothermal crystallization peaks for the glass, which were compared with experimental results. These studies allowed an investigation of the effect of the heterogeneities on the nucleation and crystallization behavior and a check on the validity of the computer model.

5.1. Nucleation rate measurements

Fig. 1(a)–(c) show the number of nuclei generated as a function of time at several representative temperatures for the undoped samples and samples containing 1 and 5 ppm of Pt, respectively. In all

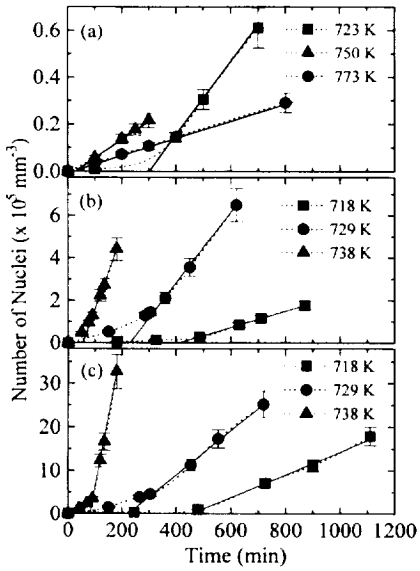

Fig. 1. Number of nuclei produced per unit volume as a function of time in $Li_2O \cdot 2SiO_2$ glass: (a) undoped, (b) glasses doped with 1 ppm and (c) glasses doped with 5 ppm platinum. Experimental errors are indicated by the error bars.

cases, the nucleation rate is very low initially and eventually reaches a steady-state value, yielding a linear rate of production of nuclei with time. The slope of the linear portion of the curve is equal to the steady-state nucleation rate, I^s; the intercept with the time axis defines the induction time for nucleation, θ. As is suggested from Fig. 1(a), homogeneous nucleation peaks at around 723 K, and the rate falls as the temperature is increased, giving smaller slopes. The induction times, however, decrease monotonically with temperature, giving a lower intercept. The heterogeneous nucleation rate peaks near 738 K.

Heterogeneous and homogeneous nucleation occur simultaneously in the doped glasses. To determine the heterogeneous nucleation rates alone, the number of nuclei generated by homogeneous nucleation was estimated from the measured homogeneous nucleation rate; this was subtracted from the total number of nuclei. The nucleation rates obtained by this method are shown in Fig. 2 as a function of temperature and dopant level. The homogeneous nucleation rates are also provided for comparison. As anticipated, the heterogeneous nucleation rates are two to three orders of magnitude larger than the homogeneous nucleation rates. Assuming that the Pt

nucleants are of similar sizes in all cases, the magnitude of the nucleation rates should scale with the density of dopants. Within measurement error, this appears to be the case here; the peak nucleation rate is approximately four to ten times larger for the 5 ppm doped sample than for the 1 ppm doped sample.

The size of the nucleating agents is important. If the heterogeneous particles are too small, their catalytic efficiency as nucleating agents is decreased [19–21]. The assumption of a flat interface between the particle and the nucleus also becomes questionable [23,24]. For particles of sufficient size, on the other hand, there is the possibility of a single nucleus supporting more than one nucleation event [24]. While the precise size of the nucleating impurity in our case is unknown, SEM studies indicate an upper bound of 100 Å for the particle size. Consequently, the average impurity size was taken as 50 Å.

Since we do not observe a decrease of the nucleation rate with time in Fig. 1, the particles are either of sufficient size to act as effective nucleating agents with no significant depletion of the heterogeneous sites during the time of our measurements or, if the heterogeneous particles are large enough to support several nucleation events, surface saturation is not important. Similar results were reported by Gonzalez-Oliver and James [22] in Pt-doped $Na_2O \cdot 2CaO \cdot 3SiO_2$ glass. In the absence of any evidence to the contrary, a single nucleation event per particle was assumed for the modeling.

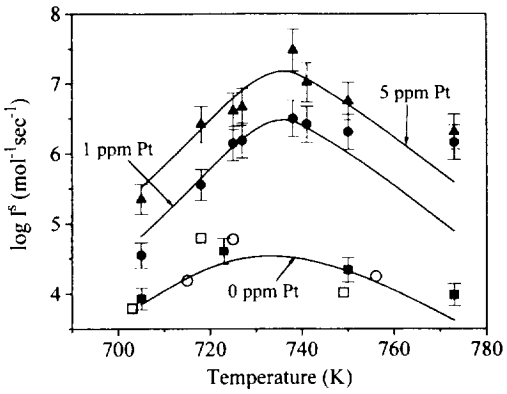

Fig. 2. Steady-state nucleation rates per mole plotted against temperature for undoped $Li_2O \cdot 2SiO_2$ (■), doped with 1 ppm Pt (●) and doped with 5 ppm Pt (▲). The solid lines are fits to the classic theory of nucleation. Homogeneous nucleation rates from Refs. [1] (□) and [3] (○) are provided for comparison.

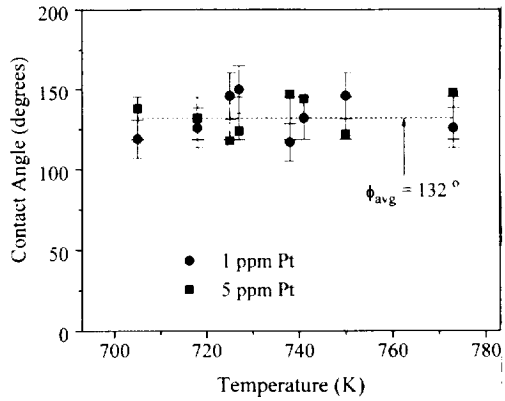

Fig. 3. The contact angle calculated from the steady-state nucleation rates using Eq. (2), for glasses doped with 1 and 5 ppm Pt.

By fitting the measured steady-state nucleation rates for the doped glasses to the classic theory of nucleation, the effective interfacial energy, σ, for the crystal and dopant interface can be obtained, which can be used to calculate the contact angle, ϕ, using Eq. (2). Shown in Fig. 3 are the calculated contact angles for the glasses containing 1 and 5 ppm Pt at different temperatures. The figure shows that ϕ is independent of both the temperature and the dopant concentration. Using the size for the catalyzing impurity, the heterogeneous nucleation rates can be described by $\phi = 132° \pm 18°$.

5.2. Induction times for nucleation

Fig. 4 compares the induction times for homogeneous nucleation, θ, with those from Refs. [1,3]. The broken line shows the calculated values [7] using the viscosity data in Ref. [25]. The good agreement between our data and those of others verifies the reliability and reproducibility of our measurements. The measured values of θ for homogeneous and heterogeneous nucleation are compared in Fig. 5. The calculated values for homogeneous nucleation are again included for comparison (solid line). Interestingly, the addition of platinum seems to have no significant effect on the induction time for nucleation.

These similarities between the measured values of θ for homogeneous and heterogeneous nucleation

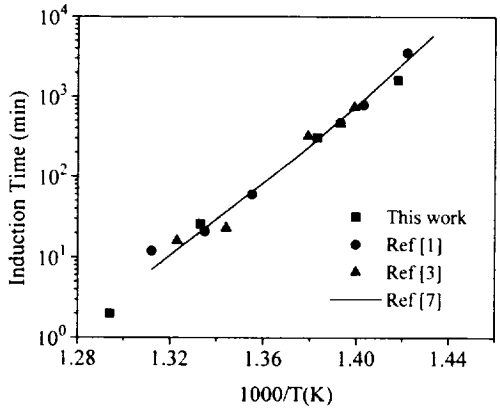

Fig. 4. The induction times for homogeneous nucleation for different temperatures. The solid line is the calculated induction time [7] using data from Ref. [24]. The experimental induction times from Refs. [1] and [3] are also included.

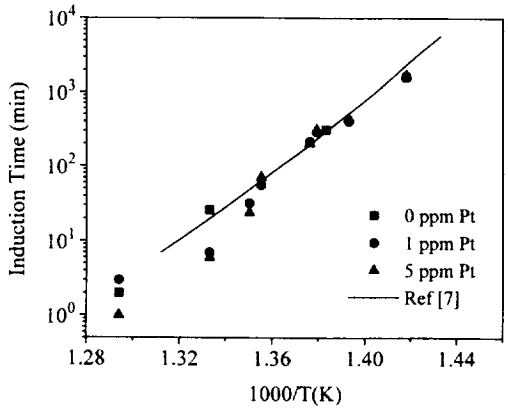

Fig. 5. The induction time for heterogeneous nucleation for glasses containing O ppm Pt, 1 ppm Pt and 5 ppm Pt. The solid line is the calculated induction time from Ref. [7].

Table 2
(a) Homogeneous crystal nucleation rates, I, and crystallization induction times, θ, for lithium disilicate

T (°C)	This work		Ref. [1]		Ref. [3]	
	I^s (mm^{-3} s^{-1})	θ (min)	I^s (mm^{-3} s^{-1})	θ (min)	I^s (mm^{-3} s^{-1})	θ (min)
430			0.368	3569		
432	0.377	1617				
440			1.147	790		
442					0.920	744
445			3.761	474		
445					1.310	461
450	2.626	308				
452					3.590	322
465			2.863	60		
471					1.610	23
476			1.868	21		
477	1.316	26				
483					1.060	16
489			0.639	12		
500	0.607	2				

(b) Crystal nucleation rates, I, and crystallization induction times, θ, for lithium disilicate glass with Pt dopants

T (°C)	$Li_2O \cdot 2SiO_2$ (1 ppm Pt by weight)		$Li_2O \cdot 2SiO_2$ (5 ppm Pt by weight)	
	I^s (mm^{-3} s^{-1})	θ (min)	I^s (mm^{-3} s^{-1})	θ(min)
432	0.6	1686	3.7	1713
445	6.1	408	43.5	443
452	23.6	289	68.4	311
454	25.9	214	78.4	203
465	52.7	56	503	71
468	43.5	32	174.8	24
477	33.7	7	93.4	6
500	23.6	3	33.8	1

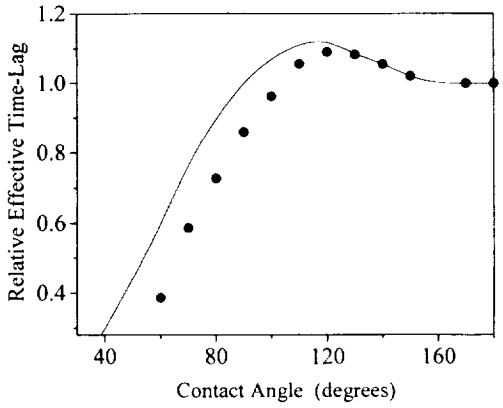

Fig. 6. Computed induction time for heterogeneous nucleation as a function of contact angle. The relative effective time-lag is defined as the ratio of $\theta(\phi)$ to $\theta(180°)$. The datapoints are from a numerical simulation; the solid line is a calculation based only on the decreased cluster surface area with decreasing contact angle. Taken from Ref. [10].

are in agreement with earlier predictions. Based on the numeric algorithm presented here, Greer et al. [10] computed the time-lag as a function of contact angle using parameters similar to those given in Table 1. The results of that calculation are shown in Fig. 6; the filled circles indicate the results of computer simulations, while the solid line is a calculation based only on the decreased interfacial area with decreasing contact angle. While a significant difference between the induction times for homogeneous and heterogeneous nucleation is predicted for small contact angles, they are nearly equal for contact angles near 130°, the value obtained for these experiments.

The measured values for θ and the steady-state nucleation rates are collected in Table 2; for comparison, data obtained by James [1] and Deubener et al. [3] are also provided. The nucleation rates and the induction times for glasses doped with 1 and 5 ppm Pt (by weight) are also provided.

5.3. Differential thermal analysis

Variations in the transformation behavior can be characterized by three parameters that describe the DTA profile: the intensity, I_p, and temperature, T_p, of the peak maximum and the peak width at half-maximum, ΔT_p. These parameters are shown as a function of platinum concentration for two DTA scan rates in Fig. 7. As demonstrated in Fig. 7(a), the peak temperature decreases approximately linearly with the logarithm of the Pt concentration, while the peak intensity increases (Fig. 7(b)) and the width decreases (Fig. 7(c)). These are expected effects. An increase in the platinum leads to an increase in the nuclei production, causing the phase transition to occur more rapidly (higher intensity) at a lower temperature than for the homogeneous case. Since the transformation occurs more quickly, it leads to a decreased peak width.

The simulation discussed in Section 3 was used to model the DTA data for lithium disilicate glass, taking the measured value for the contact angle, ϕ, and the known values for the free energy, interfacial energy and the diffusion coefficient (Table 1). The DTA peak parameters determined from the computed peaks are indicated by the solid lines in Fig. 7.

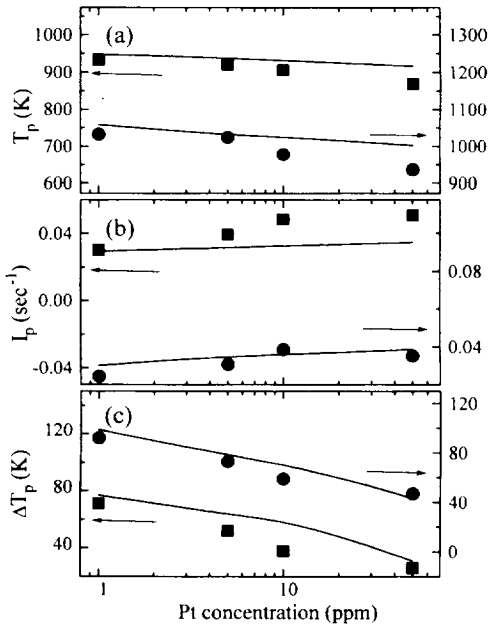

Fig. 7. Plot of characteristic DTA peak parameters as a function of the dopant concentration at scan rates of 5 K/min (■) and 80 K/min (●). The left vertical axes correspond to the 5 K/min values; the right vertical axes correspond to the 80 K/min values. (a) Temperature of the peak rate of transformation; (b) normalized peak intensities; and (c) full width at half-maximum. The solid lines are the calculated values based on the parameters extracted from the nucleation rate measurements.

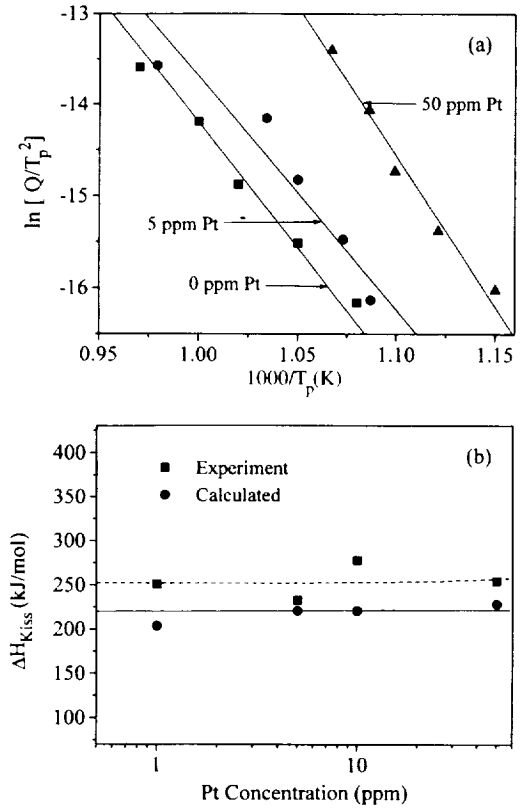

Fig. 8. Kissinger analysis for samples with different dopant concentrations. (a) Typical Kissinger plots for glasses doped with 0, 5 and 50 ppm Pt. (b) Activation energies determined from the Kissinger plots of experimental (■) and computed (●) DTA peaks. The lines are straight line fits to the points.

Differential scanning calorimetry and DTA data are typically analyzed using the Kissinger method [26]. The slope of $\ln[Q/T_p^2]$ vs. $1/T_p$, at which Q is the heating rate and T_p is the temperature of the DTA peak maximum, is argued to give the activation energy of the transformation. Fig. 8 shows the experimental DTA data analyzed in that way. A series of straight lines are obtained with slopes roughly independent of the platinum concentration. The slopes of these lines give activation energies between 250 and 275 kJ/mol, which are in reasonable agreement with previously reported values for this glass [29–31]. The simulated DTA peaks obtained at different heating rates were also analyzed by the Kissinger method. As shown in Fig. 8(a), the activation energies calculated from the simulated data are slightly lower than the values computed from the experimental data, although the differences were within 20–40 kJ/mol. The good agreement between the model calculations and the experimental data shown in Figs. 7 and 8 demonstrates the validity of our modeling approach and justifies the usefulness of such computer calculations for analyzing DSC and DTA data.

The activation energies determined from the Kissinger method are close to the value for macroscopic growth in lithium disilicate glass (282 kJ/mol) [27]. This supports previous suggestions that the Kissinger analysis provides a reasonable estimate of the activation energy for growth [32], but should not be taken to describe the overall activation energy of the transformation. Consequently, caution should be exercised when applying the Kissinger analysis to first order phase transformations proceeding by nucleation and growth. The numerical approach presented here provides a better basis for analysis.

6. Conclusions

Our results are in good agreement with predictions based on the classic theory of nucleation and with previous computer models of heterogeneous nucleation. The induction times for homogeneous and heterogeneous nucleation are virtually identical, which agrees with previous predictions that the induction time for heterogeneous nucleation approaches that for homogeneous nucleation when the contact angle is high (120–130°), the value extracted from the measured heterogeneous nucleation rates. A computer model of non-isothermal phase transformations in heterogeneously nucleating glasses is developed and demonstrated to give good agreement with experimental data, pointing to a more quantitative approach to the analysis of such data.

Acknowledgements

The authors thank D.E. Day, A.L. Greer and M. Weinberg for useful discussions. This work was partially supported by NASA under contracts NAG 8-873, NCC 8-49, and NAG 8-898.

References

[1] P.F. James, Phys. Chem. Glasses 15 (1974) 95.
[2] A.M. Kalinina, V.N. Filipovich and V.M. Fokin, J. Non-Cryst. Solids 38&39 (1980) 723.
[3] J. Deubener, R. Brückner and M. Sternitzke, J. Non-Cryst. Solids 163 (1993) 1.
[4] JANAF Thermochemical Tables, 2nd Ed., US Department of Commerce, National Bureau of Standards, Washington, DC, 1971.
[5] K.F. Kelton, A.L. Greer and C.V. Thompson, J. Chem. Phys. 79 (1983) 6261.
[6] K.K. Kelton and A.L. Greer, Phys. Rev. B38 (1988) 10089.
[7] K.F. Kelton and M.C. Weinberg, J. Non-Cryst. Solids 180 (1994) 17.
[8] K.F. Kelton and A.L. Greer, J. Non-Cryst. Solids 79 (1986) 295.
[9] K.F. Kelton, J. Non-Cryst. Solids 163 (1993) 283.
[10] A.L. Greer, P.V. Evans, R.G. Hamerton, D.K. Shangguan and K.F. Kelton, J. Cryst. Growth 99 (1990) 38.
[11] M.C. Weinberg, J. Non-Cryst. Solids 122 (1990) 139.
[12] G. Rindone, J. Am. Ceram. Soc. 41 (1958) 41.
[13] D. Cronin and L. Pye, J. Non-Cryst. Solids 84 (1986) 196.
[14] A.L. Greer and K.F. Kelton, J. Am. Ceram. Soc. 74 (1991) 1015.
[15] P.F. James, in: Glasses and Glass-Ceramics, ed. M.H. Lewis (Chapman and Hall, London, 1989) p. 59.
[16] D. Turnbull and J.C. Fischer, J. Chem. Phys. 17 (1949) 71.
[17] K.F. Kelton and A.L. Greer, in: Proc. 5th Int. Conf. on Rapidly Quenched Metals, Wurzburg, ed. S. Steed and H. Warlimont (North-Holland, Amsterdam, 1985) p. 223.
[18] E.E. Underwood, Quantitative Stereology (Addison–Wesley, New York, 1970).
[19] R.D. Maurer, J. Chem. Phys. 31 (1959) 444.
[20] I. Gutzow and S. Toschev, in: Advances in Nucleation and Crystallization in Glasses, ed. L.L. Hench and S.W. Freiman (American Ceramic Society, Westerville, OH, 1971) p. 10.
[21] I. Gutzow, Contemp. Phys. 21 (1980) 121; 243.
[22] C.J.R. Gonzales-Oliver and P.F. James, in: Advances in Ceramics, Vol. 4, ed. J.H. Simmons, D.R. Uhlmann and G.H. Beall (American Ceramic Society, Columbus, OH, 1982) p. 49.
[23] N.H. Fletcher, J. Chem. Phys. 31 (1959) 1136.
[24] C.J.R. Gonzalez-Oliver and P.F. James, J. Microsc. 119 (1980) 73.
[25] K. Matusita and M. Tashiro, Jpn. J. Ceram. Assoc. 81 (1973) 500.
[26] H.E. Kissinger, J. Res. Nat. Bur. Stand. 57 (1956) 217.
[27] M.F. Barker, T. Wang and P.F. James, Phys. Chem. Glasses 29 (1988) 240.
[28] J.W. Christian, The Theory of Transformation in Metals and Alloys, 2nd. Ed. (Pergamon, Oxford, 1975) ch. 10.
[29] C.S. Ray and D.E. Day, J. Am. Ceram. Soc. 73 (1990) 439.
[30] A. Marotta, A. Buri, F. Branda and S. Saiello, in: Advances in Ceramics, Vol. 4, ed. J.H. Simmons, D.R. Uhlmann and G.H. Beall (American Ceramic Society, Columbus, OH, 1982) p. 146.
[31] P. Hautojarvi, A. Vehanel, V. Kompa and E. Pahane, J. Non-Cryst. Solids 29 (1978) 365.
[32] H. Yinnon and D.R. Uhlmann, J. Non-Cryst. Solids 54 (1983) 253.

Journal of Non-Crystalline Solids

Instructions to Authors

Submission of papers

Manuscripts (one original + two copies), should be sent to the editors or any one of the regional editors. The address of the editors is as follows:

Profs. R.A. Weeks and D.L. Kinser
Editors, Journal of Non-Crystalline Solids
Vanderbilt University, 610 Olin Hall
Nashville, TN 37540, USA.
Fax: +1-615 343 8645.
E-mail: jncs@vuse.vanderbilt.edu

Original material: On submission, authors are asked to confirm that the manuscript is not being simultaneously considered for publication elsewhere and that all authors have approved the manuscript and take full responsibility for its contents and so state in their letter of transmittal.

Types of contributions

Original research papers, reviews, letters to the editor and commentaries are welcome. They should contain an Abstract (of up to 200 words) and a Conclusions section which, particularly in the case of theoretical papers, translates the results into terms readily accessible to most readers.

Letters should be no longer than six double-spaced typed pages. They will be given priority in both the refereeing and production processes. The faster production schedule will preclude sending proofs of letters to authors.

Manuscript preparation

All manuscripts should be written in good English. The paper copies of the text should be prepared with double line spacing and wide margins, on numbered sheets. See notes opposite on electronic version of manuscripts.

Structure. Please adhere to the following order of presentation: Article title, Author(s), Affiliation(s), Abstract, PACS codes, Main text (Introduction; Experimental procedures or constraints on theory; Results; Discussion; Conclusion. Sections and sub-sections must be clearly numbered according to the Journal style), Acknowledgements, Appendices, References, Figure captions, Tables.

Corresponding author. The name, complete postal address, telephone and fax numbers and the e-mail address of the corresponding author should be given on the first page of the manuscript.

PACS codes/keywords. Please supply one or more relevant PACS-1995 classification codes.

References. References to other work should be consecutively numbered in the text using square brackets and listed by number in the Reference list. Please refer to past issues of the Journal for examples.

Symbols/Units: Authors should follow the Symbols and Units Nomenclature Commission of the I.U.P.A.P. (Physica 146A (1987) 1–68).

Illustrations (figures)

Illustrations should also be submitted in triplicate: one master set and two sets of copies. The *line drawings* in the master set should be original laser printer or plotter output or drawn in black india ink, with careful lettering; lettering should 2 mm in height after reduction for printing. The *photographs* should be originals, with somewhat more contrast than is required in the printed version. The top edge should be indicated on the back. They should be unmounted unless part of a composite figure. Any scale markers should be inserted on the photograph itself, not drawn below it.

Colour plates. Figures may be published in colour, if this is judged essential by the editor. The publisher and the author will each bear part of the extra costs involved. Further information is available from the publisher.

After acceptance

Notification. You will be notified by the Editor of the journal of the acceptance of your article and invited to supply an electronic version of the accepted text, if this is not already available.

Copyright transfer. In the course of the production process you will be asked to transfer the copyright of the article to the publisher. This transfer will ensure the widest possible dissemination of information.

IMPORTANT: When page proofs of the accepted manuscript are made and sent to authors, this is in order to check that no undetected errors have arisen in the typesetting (or file conversion) process. Only printers' errors may be corrected; no changes in, or additions to, the edited manuscript will be accepted. In the case of extended changes, the authors will be required to pay part of the extra costs involved.

Electronic manuscripts

The publisher welcomes the receipt of an electronic version of your accepted manuscript. If there is not already a copy of this (on diskette) with the journal editor at the time the manuscript is being refereed, you will be asked to send a file with the text of the accepted manuscript directly to the Publisher by e-mail or on diskette (allowed formats 3.5″ or 5.25″ MS-DOS, or 3.5″ Macintosh) to the address given below. Please note that no deviations from the version accepted by the Editor of the journal are permissible without the prior and explicit approval by the Editor. Such changes should be clearly indicated on an accompanying printout of the file.

Author benefits

No page charges. Publishing in Journal of Non-Crystalline Solids is free.

Free offprints. The corresponding author will receive 50 offprints free of charge. An offprint order form will be supplied by the publisher for ordering any additional paid offprints.

Discount. Contributors to Elsevier Science journals are entitled to a 30% discount on all Elsevier Science books.

Further information (after acceptance)

Elsevier Science B.V.
Journal of Non-Crystalline Solids
Desk Editorial Department
P.O. Box 103, 1000 AC Amsterdam
The Netherlands.
Fax: +31 20 485 2775.
E-mail: g.anderton@elsevier.nl

North-Holland, an imprint of Elsevier Science